

FA7 AFBSD-

CG

CER 63-80

COPY 2

~~SECRET~~  
ENGINEERING RESEARCH

JUL 3 '69

RESEARCH AND ADVANCED DEVELOPMENT DIVISION

MEASUREMENT OF HEAT TRANSFER ON A FLAT PLATE-STEP  
MODEL AT MACH 14  
(Task 3.4--Shock Tunnel Experiments--REST Project)

Prepared by

V. A. Sandborn  
K. Heron

RESEARCH AND ADVANCED DEVELOPMENT DIVISION  
AVCO CORPORATION  
Wilmington, Massachusetts

Technical Memorandum

RAD-TM-63-40

Contract AF04(694)-239

THIS REPORT WAS PREPARED IN ACCORDANCE WITH AIR FORCE  
CONTRACT NUMBER AF04(694)-239. IT IS SUBMITTED IN PAR-  
TIAL FULFILLMENT OF THE CONTRACT AND IN ACCORDANCE  
WITH AFBM EXHIBIT 58-1 (PARAGRAPH 4.2.1).

26 June 1963

Prepared for

AIR FORCE BALLISTIC SYSTEMS DIVISION  
AIR FORCE SYSTEMS COMMAND  
UNITED STATES AIR FORCE  
Norton Air Force Base, California

CER63 VAS 80 ✓

MEASUREMENT OF HEAT TRANSFER ON A FLAT PLATE-STEP  
MODEL AT MACH 14  
(Task 3.4--Shock Tunnel Experiments--REST Project)

Prepared by

V. A. Sandborn  
K. Heron

RESEARCH AND ADVANCED DEVELOPMENT DIVISION  
AVCO CORPORATION  
Wilmington, Massachusetts

Technical Memorandum

RAD-TM-63-40

Contract AF04(694)-239

THIS REPORT WAS PREPARED IN ACCORDANCE WITH AIR FORCE  
CONTRACT NUMBER AF04(694)-239. IT IS SUBMITTED IN PAR-  
TIAL FULFILLMENT OF THE CONTRACT AND IN ACCORDANCE  
WITH AFBM EXHIBIT 58-1 (PARAGRAPH 4.2.1).

26 June 1963

APPROVED

H. Weisblatt  
H. Weisblatt, Project Engineer  
Shock Tunnel Experiments

J. Luceri  
J. Luceri, Manager  
REST Project Office

Prepared for

AIR FORCE BALLISTIC SYSTEMS DIVISION  
AIR FORCE SYSTEMS COMMAND  
UNITED STATES AIR FORCE  
Norton Air Force Base, California



U18401 0573966

## SUMMARY

An experimental study of the separation of a hypersonic boundary layer ahead of a step on a flat plate is reported. The measurements were made in a Mach 14 shock tunnel. The flow field is visually observed with a glow probe. Local heat transfer distribution along the flat plate and up the face of the step is reported. The detailed heat transfer distribution shows a local increase in heat transfer associated with the separation shock, a decrease in heat transfer just downstream of the separation point, and a second increase in heat transfer as the step is approached. Directly at the corner between the flat plate and the step, the heat transfer reverses direction and is from the heat gage to the stream. No explanation was found for the corner effect. Preliminary measurements of the local heat transfer distribution across the separation layer with hot wire calorimeters are also reported.

CONTENTS

I.	Introduction.....	1
II.	Test Setup and Procedure.....	2
	A. Shock Tunnel.....	2
	B. Model.....	2
	C. Flow Visualization.....	3
	D. Surface Heat-Transfer Measurements.....	4
	E. Hot-Wire Heat-Transfer Measurements.....	4
III.	Results and Discussion.....	13
	A. Observation of the Separated Region.....	13
	B. Local Heat-Transfer Distribution Across the Separated Region.....	15
IV.	Concluding Remarks.....	28
V.	References.....	29
	Appendix	
	The Hot-Wire Calorimeter.....	30

ILLUSTRATIONS

Figure 1	Photograph of Shock Tunnel Test Section and Data Console .....	6
2	Shock Tunnel Dimensions .....	7
3	Schematic Diagram of Model Mounted in the Test Section of the Shock Tunnel.....	7
4	Reservoir Measurements .....	8
5	Glow Probe.....	9
6	Set of Ten Thin Film Heat Transfer Gages .....	9
7	Thin Film Heat Transfer Gage Electrical Circuit.....	10
8	Constant Current Hot Wire Circuit.....	10
9	Hot Wire Calorimeters Mounted on Model .....	11
10	Schlieren Time History Study of Separation Development .....	17
11	Carbon Black Flow Visualization in the Region of the Step. Shock Tunnel Flow Conditions.....	18
12	Shock Wave Structure Indicated from Glow Probe Photograph.....	19
13	Plot of Theoretical and Experimental Heat Transfer Distribution on a Flat Plate .....	20
14	Plot of Theoretical Experimental Heat Transfer Distribution on a Flat Plate .....	21
15	Plot of Experimental Heat Transfer Distribution on a Flat Plate with Step .....	22
16	Plot of Experimental Heat Transfer Distribution on a Flat Plate with a Forward Facing Step .....	23
17	Distribution of Heat Transfer on Face of Step .....	24

ILLUSTRATIONS (Concl'd)

Figure 18	Model Flow Field in Separated Region.....	25
19	Typical Output Traces from the Hot Wire Probes and a Heat Gage .....	26
20	Measurements of the Local Heat Transfer Across the Separated Layer (1.5 inches ahead of the step).....	27

## SYMBOLS

C	Specific heat of wire material (for tungsten $C = 0.128$ joules/ $\text{gm}^\circ\text{K}$ )
D	Wire diameter (0.00127 cm)
E	Voltage output of hot wire (volts)
$h_{ST}$	Enthalpy, stagnation (cal/gm)
$h_W$	Enthalpy, wall (cal/gm)
i	Heating current through the hot wire (amp)
k	Thermal conductivity of wire material (for tungsten $k = 160.2$ W/ $\text{m}^\circ\text{K}$ )
$l$	Wire length (cm)
Nu	Nusselt Number
Pr	Prandtl Number
q	Local heat transfer rate (watts/ $\text{cm}^2$ )
$q_t$	Sum of local and convective heat transfer rates (watts/ $\text{cm}^2$ )
$q_c$	Conduction heat transfer rate for the hot wires (watts/ $\text{cm}^2$ )
Re	Reynolds Number
$R_o$	Wire resistance at $273^\circ\text{K}$ (ohms)
T	Temperature ( $^\circ\text{K}$ )
t	Time (seconds)
x	Distance (cm)
$\alpha$	Thermal coefficient of resistance for the hot wire ( $1/^\circ\text{K}$ ) (for tungsten $\alpha = 4 \times 10^{-3}/^\circ\text{K}$ )
$\rho$	Density of hot wire material (for tungsten $\rho = 19.50$ gm/ $\text{cm}^3$ )
$\mu$	Viscosity of air

## I. INTRODUCTION

Of the many viscous flow problems associated with hypersonic vehicles, the separated flow region is the least understood. Both the separation of the boundary layer in rising pressure regions and the trailing wake behind the vehicle require a great deal of study. Even for the incompressible case the separated flow region cannot be treated theoretically. Theoretical solutions, such as exist, fail even before separation is reached and empirical relations are employed to predict the point of separation.<sup>1</sup> Present empirical analysis are no better than the theoretical solutions, as curve fitting is employed to predict separation when the empirical solutions reduce to one unique point at separation.<sup>2</sup> The general approach, which is certainly adequate for boundary layers far from separation, of using a one parameter representation of the boundary layer simply is not valid near separation.

Inroads have been made into understanding the boundary layer near separation.<sup>3</sup> However, results at present are limited to correlating the measurements, and no engineering predictions have yet been possible. By simply abandoning a one parameter approach to representing the boundary layer a consistent model of separation is obtained. Further, it is possible to demonstrate that two types of separation exist; either steady or unsteady. In other words, there is no unique difference in velocity profile shape between a steady laminar separation and a "steady" turbulent separation, or an "unsteady" laminar separation and an "unsteady" turbulent separation. Experimental measurements are in good agreement with correlations predicted from the model.

Although still limited by the one parameter assumptions, it has been demonstrated that integral equations can be used downstream of the separation point.<sup>4</sup> Thus, the application of integral equations with more realistic boundary layer representation should lead to useable engineering predictions of the separated flow region. Still lacking the engineering predictions, it is necessary to experimentally determine the flow characteristics in the separation region. The present experimental study was undertaken to provide data on separated flow fields at conditions more closely approaching reentry simulation. Limited data on separated flow is available up to about Mach 6, but none exists at either flow conditions or Mach numbers approaching reentry conditions.

## II. TEST SETUP AND PROCEDURE

### A. SHOCK TUNNEL

The tests were made in the test section of a 20-inch-diameter shock tunnel. A photograph of the test section together with the tunnel data console is shown in figure 1. The shock tunnel is a blow-down type tunnel which uses a shock tube to create a very high temperature--high-pressure gas reservoir conditions. Specific dimensions of the present shock tunnel are given in figure 2. A high pressure driver section 3-feet long, together with a driver sphere<sup>5</sup> is filled with 1600 lb/in.<sup>2</sup> of hydrogen to drive a shock wave down the 15-foot driver section. A diaphragm separates the driver and driver section before the run. The diaphragm is prescribed, and the driver section is loaded with hydrogen until the diaphragm ruptures. The driver section contained air at 100- or 120-mm Hg absolute pressure. A "milar" diaphragm separates the shock tube from the tunnel nozzle and test section. The tunnel test section was evacuated to approximately  $10^{-3}$  mm Hg pressure before each run. A schematic diagram of the tunnel test section is shown in figure 3.

The shock wave created by the ruptured diaphragm travels down the shock tube and is reflected back at the milar diaphragm creating a stagnate region of high temperature--high-pressure air. When the milar diaphragm ruptures the reservoir gas is expanded through the nozzle into the test section. Figure 4 shows oscilloscope traces of the shock wave speed down the shock tube, the pressure-time history in the reservoir, the optical radiation-time history in the reservoir, and an electron-collector indication of the electron density variation with time in the reservoir. The shock tube was operated at tailored conditions,<sup>5</sup> so approximately 2 ms of steady reservoir conditions were obtained. For the present tests, the nominal reservoir conditions are given in table I.

Based mainly on pressure and heat-transfer measurements on the surface of a cone,<sup>6</sup> it was determined that the conditions in the test section are those listed in table I. The flat plate measurements presented in the present report appear to confirm the cone predictions. Total pressure measurements show a test core of 12 inches is available.<sup>6</sup> Within the accuracy of the measurements, the flow appears to be uniform over the 12-inch test core. A slight drop in total pressure appears to occur with distance downstream, however, it is within the uncertainty of the measurements.

### B. MODEL

A schematic diagram of the specific models used in the present program is shown as an insert in figure 3. Two actual models were employed in the present measurements. The surface heat-transfer model shown in figure 3 was of steel with a plastic (lucite) step. The leading edge radius was estimated from microscope observations as 0.001 inch. A second flat-plate model identical in dimensions

was used for the hot-wire measurements. This model was made of brass with a lucite surface starting 1 inch behind the leading edge and extending back to the step. The lucite surface is not thought to be of importance in the present experimental program, and is intended for use when the electromagnetic properties of the separated flow are measured. The leading edge radius for the brass-lucite model was estimated as 0.0005 inch.

### C. FLOW VISUALIZATION

Several techniques were experimentally employed to help define the flow field above the flat, plate-step configuration. To understand the time history of the flow (necessary in interpreting the traces from transducers) a time history schlieren study was made on a small model in the 1.5-inch-diameter shock tube. The schlieren system was a single pass with a horizontal knife edge. A spark of approximately 5- $\mu$  sec duration was used as the light source. The spark source was "fired" at a predetermined time by triggering a time-delay generator with the output from a speed box upstream of the test section.

Because of the extreme low density in the shock tunnel test section, a schlieren system could not be employed. The first attempts to obtain an indication of the flow distribution along the model was to use a lamp black-oil trace technique. Again the density proved to be too low, so that the shear forces were too small to move the coating. Small drops of jewelers oil gave some evidence of flow direction, but were still inconclusive. A very light coat of soot (carbon) produced with a welding torch held below the inverted model proved to be the best indicator of the flow field. Shear forces on the face of the step and for a short distance directly in front of the step were sufficient to move the soot. The direction of flow in the boundary layer ahead of separation was indicated by a few streaks in the soot. The impression was that solid particles may have been the cause of the streaks. At a distance of approximately 2-1/2 to 3 inches from the step, no disturbance to the soot could be observed. From the soot observations it was suspected that separation was occurring in the neighborhood of 3 inches ahead of the step. Use of talcum powder, as an indicator, gave much the same results as the carbon, but in each case the indicator was by no means adequate to define the flow along the surface. No evidence of secondary flows from the edges could be seen with the visualization techniques.

The third approach to observe the flow above the model was the use of a glow probe. The glow probe has been used in low density, low temperature, continuous flow hypersonic-wind tunnels. However, no reference to its use in shock tunnels was found. A solid brass cone 1-15/16-inches long and 0.615-inch in diameter at its base was used as the glow probe. A photograph of the probe is shown in figure 5. The glow probe was operated at -1150 volts with respect to the model, which was grounded to the shock tunnel. The probe was mounted about 3-1/2-inches above the model with its tip about an inch behind the model leading edge. Only the steel model proved useable with the glow probe. The glow was recorded with a portrait camera. The technique proved feasible, but the short duration of flow and low-light intensity made the glow difficult to

photograph. Attempts to use a 10-inch diameter spherical mirror, to produce a sharp focused picture of the plate and step without parallax, had to be abandoned because of the loss of light. The portrait camera, with a 3-inch diameter, 18-inch focal-length lens, was set at a distance of 56 inches from the centerline of the tunnel for the photograph reported herein; it was necessary to use Polaroid Land 3000 speed film to record the glow. The photograph is an integrated picture over the complete time the glow exists. The camera is simply opened (before the run) into the completely dark tunnel test section, and closed after the run was completed. No evidence on the exact time the flow starts or ends is available at the present time. The present use of the glow probe data must be viewed as preliminary, and in part it demonstrates (apparently for the first time) the feasibility of using it as a visualization in shock tunnel flow investigations.

#### D. SURFACE HEAT-TRANSFER MEASUREMENTS

A comparison of the heat-transfer distribution for a flat plate and for the same flat plate with a separation flow region created by a forward facing step enable the region in which separation occurs to be identified. The technique described below also makes possible a detailed study of the heat transfer to the surfaces in the separated region.

The heat transfer to the surface was measured using thin film platinum resistance thermometers deposited on microscope slides which were mounted in the surface of the model. Figure 6 is a photograph of one of the slides containing 10 gages. Each gage consisted of five hand-painted coats of platinum paint, (No. 1X from Hanovia Chemical and Manufacturing Co., 1 West Central Avenue, East Newark, N. J.) with each coat individually fired in a furnace. The temperature of the furnace was slowly brought up to 1260° F and then allowed to cool slowly to room temperature. Two potential and two current leads (28-gage copper wire) were connected to each thin film gage through 0.02-inch-diameter holes drilled through the microscope slide. Electronic-grade solder (2 percent silver) with a melting point near 233° F was used to secure the connections. The finished gage was approximately  $8 \times 10^{-6}$  inch thick and 0.025-inch wide by 0.15-inch long; its resistance was approximately 50 ohms. The solder connections extended above the surface by about  $5 \times 10^{-4}$  inch. A photomicrograph of a typical thin-film gage is shown in figure 6.

Each gage was calibrated by subjecting it to a known step change in current and by measuring the voltage change across the film as described in reference 7. Any gage with a calibration constant outside a certain range was not used. The operating circuit for a bank of five gages is shown in figure 7.

The methods of reference 8 were used in the data reduction procedure.

#### E. HOT-WIRE HEAT-TRANSFER MEASUREMENTS

Preliminary measurements of the local heat transfer distribution from 0.0005-inch diameter tungsten wires were made at one station in the separated flow

region. The wires were approximately 0.08-inch long. The wires were operated by simple constant current circuits shown in figure 8. The wire supports were mounted in the model step as shown in figure 9. The supports which are soft steel 0.045 inch in diameter, tapered to approximately 0.02 inch at the tip, extended to a point 1.5 inches ahead for the step. The wires are staggered across the model span, so that a minimum of disturbance can be caused at any one point. Because of the very low density in the tunnel, no difficulty was encountered due to support vibration or wire breakage.

The application of hot wires to measurements in shock tunnels has not previously been reported, therefore, the present measurements must be regarded as preliminary. A brief discussion of the theory and evaluation of the hot-wire measurements is given in the appendix. The brass model with the lucite insert was used for the hot-wire measurements. The model and particular wires employed were specifically chosen for the electromagnetic studies (not reported in the present paper), so they do not necessarily represent the optimum measuring instruments.

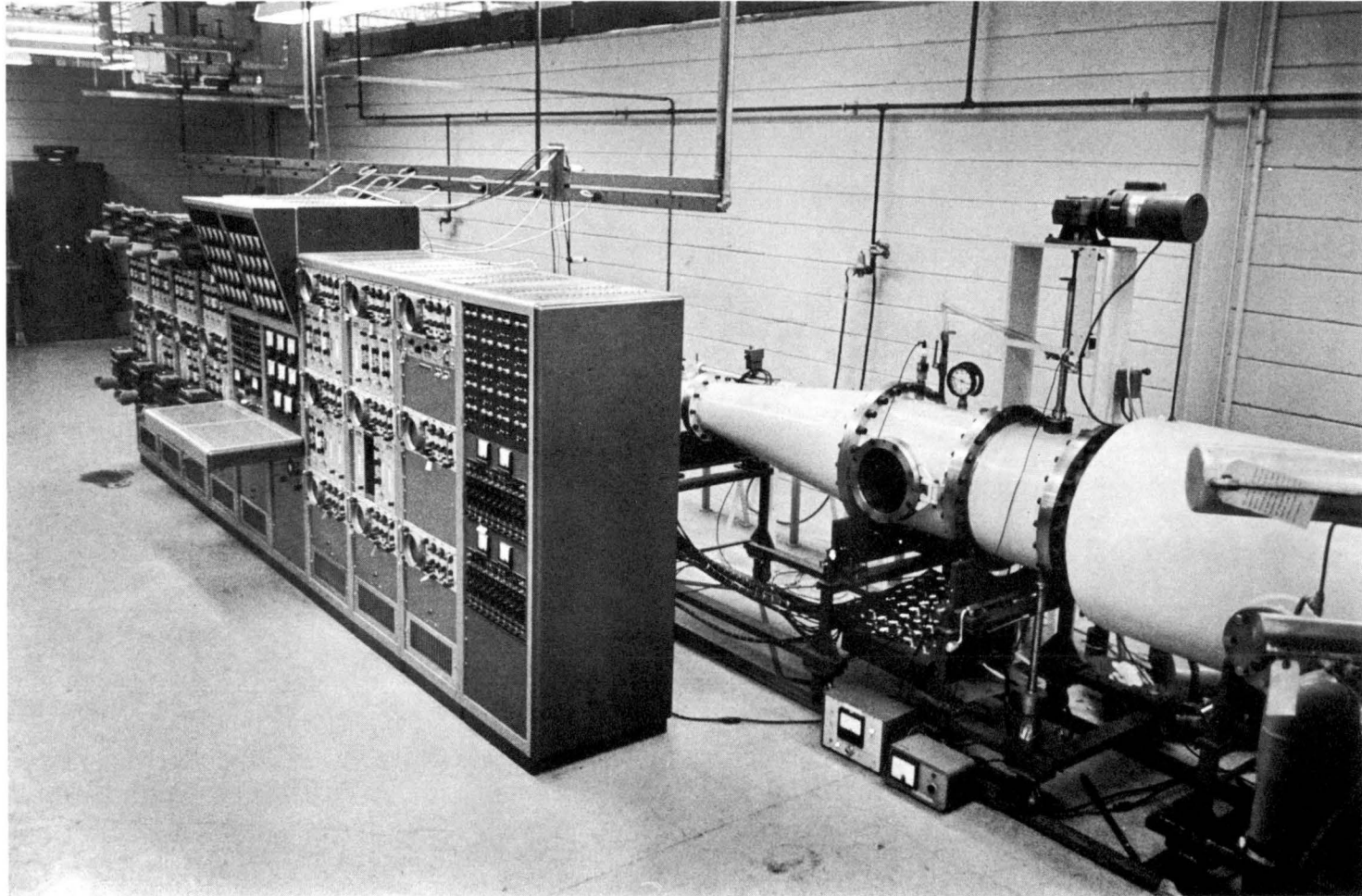


Figure 1 PHOTOGRAPH OF SHOCK TUNNEL TEST SECTION AND DATA CONSOLE

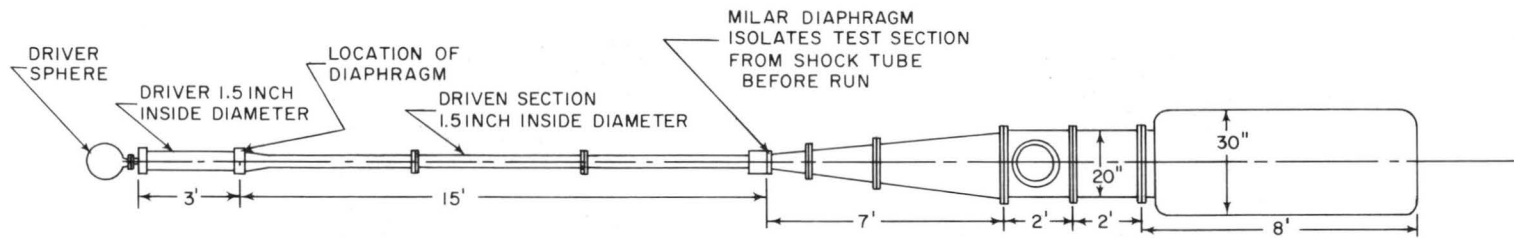


Figure 2 SHOCK TUNNEL DIMENSIONS  
63-5447

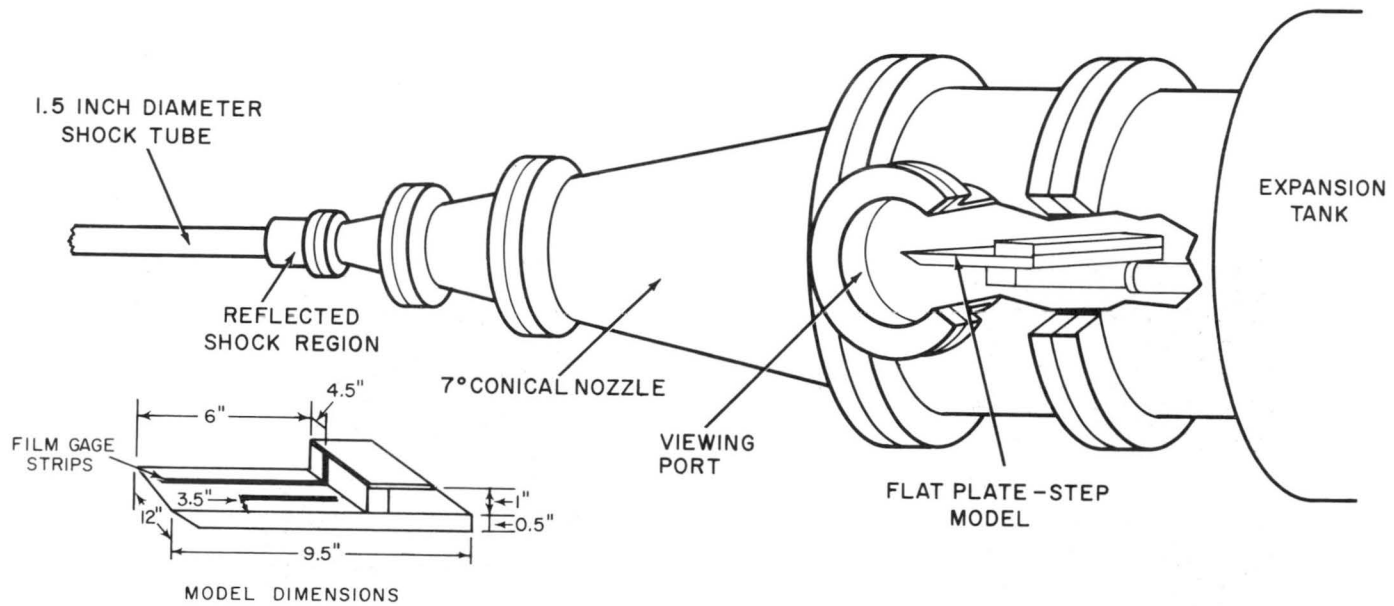
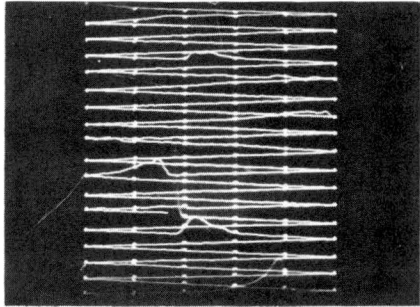
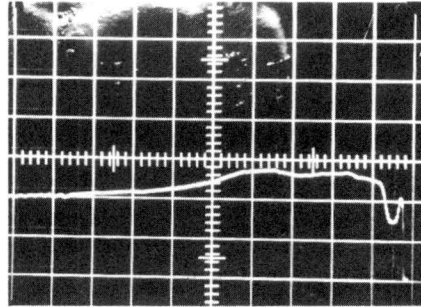


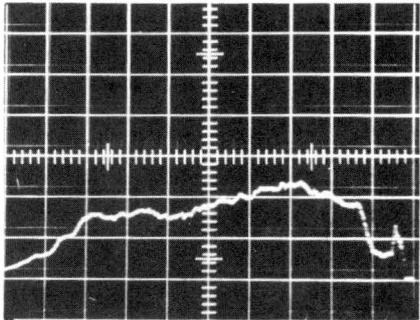
Figure 3 SCHEMATIC DIAGRAM OF MODEL MOUNTED IN THE TEST SECTION  
OF THE SHOCK TUNNEL  
63-5447



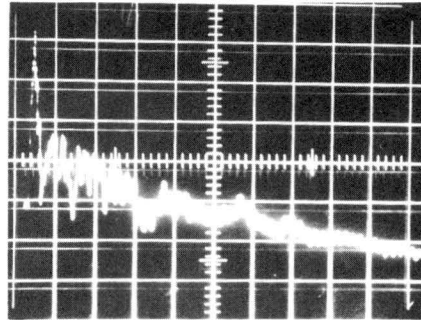
SHOCK VELOCITY



← TIME  
PRESSURE



← TIME  
RADIATION



TIME →  
ELECTRON COLLECTOR

Figure 4 RESERVOIR MEASUREMENTS  
63-5448

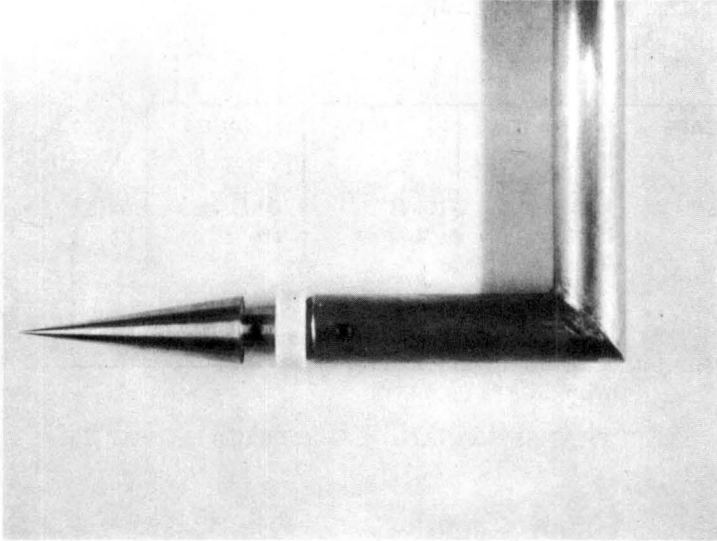


Figure 5 GLOW PROBE  
63-5449

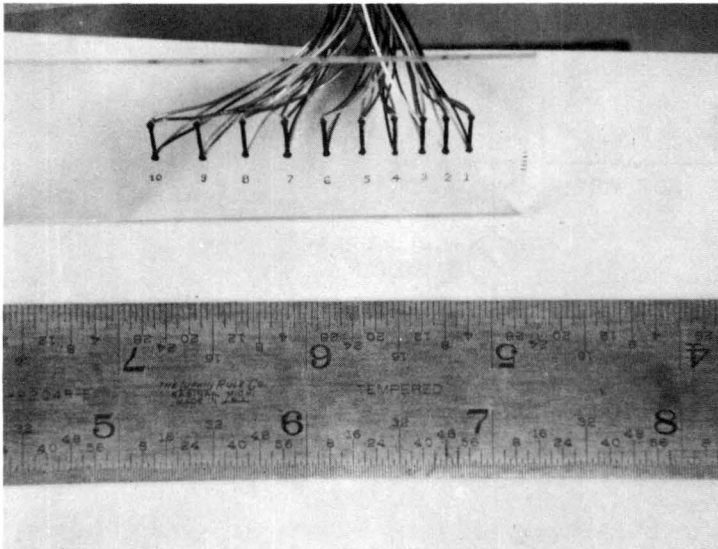
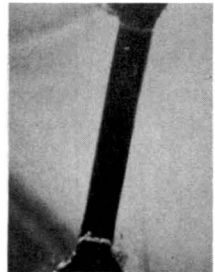


Figure 6 SET OF TEN THIN FILM HEAT TRANSFER GAGES  
63-5449



PHOTOMICROGRAPH  
OF A SURFACE GAGE  
WIDTH 0.026 inch  
LENGTH 0.150 inch

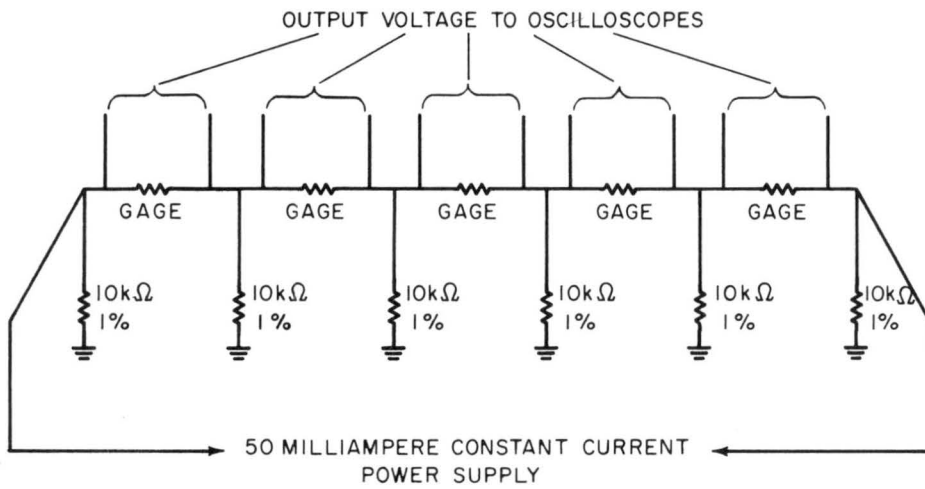


Figure 7 THIN FILM HEAT TRANSFER GAGE ELECTRICAL CIRCUIT  
63-5450

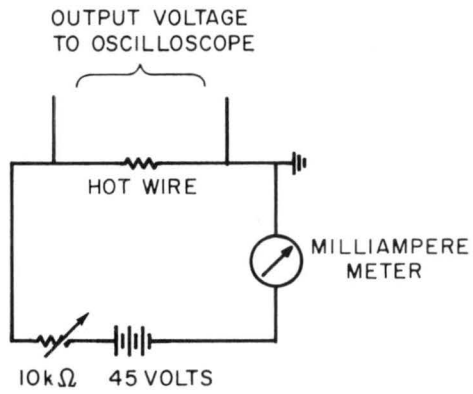


Figure 8 CONSTANT CURRENT HOT WIRE CIRCUIT  
63-5450

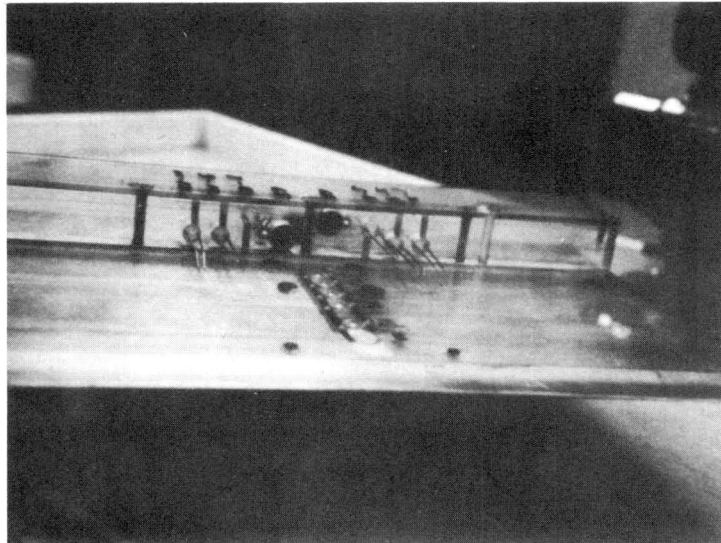
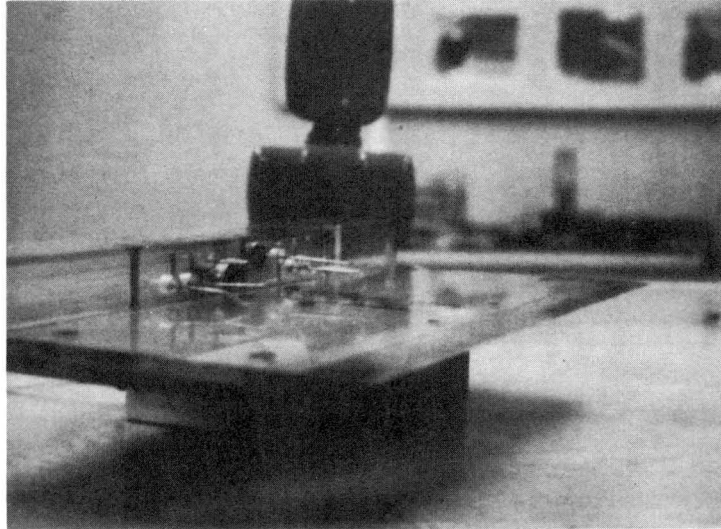


Figure 9 HOT WIRE CALORIMETERS MOUNTED ON MODEL  
63-5451

TABLE I

TEST CONDITIONS

Initial Shock Tube Pressure (psia)	Shock Tube Mach No.	Reflected Shock (Reservoir) Pressure (psia)	Reflected Shock (Reservoir) Temperature (°K)	Tunnel Flow Mach No.	Static Pressure (psia)	Static Temperature (°K)	Reynolds Number Per Foot
2.3	6.2	850	3576	~ 14	0.001	120	$2.4 \times 10^4$
1.9	6.3	770	3688	~ 14	0.001	126	$1.6 \times 10^4$

### III. RESULTS AND DISCUSSION

#### A. OBSERVATION OF THE SEPARATED REGION

At the outset of the present separated flow studies, it was planned to explore the separation ahead of steps in both shock tube and tunnel flows. Unfortunately, schlieren studies of the shock tube flow over a flat plate with a step indicates that the shock reflected from the tube walls may be affecting the flow field. Thus, the shock tube studies were not extended beyond the schlieren studies. Figure 10 shows a "time history" schlieren study made of the separation development. This study proved of value in understanding the time history of a thin film gage output in the separation region. The film gage should show a heat-transfer rate corresponding to a developing flat-plate boundary layer after the shock passes, and then when the "reflected" separation shock travels back along the plate a new heat-transfer rate would appear.

For visual studies of the separation in the shock tunnel both surface indicators (soot) and the glow probe technique were employed. Figure 11 is a top-view photograph of the flat-plate step model after a run in the shock tunnel. The model was originally all black with soot. The light region shown on figure 11 shows where the soot has been blown away. Minute streaks, which were too small to show on figure 11, were observed ahead and behind a region some 2-1/2 to 3 inches ahead of the step. The normal interpretation of a surface indicator is that regions of high shear remove the indicator. This means that the region directly in front of the step must be a region of high shear. Also the shear in the region must be greater than the normal flat-plate boundary layer shear, since no evidence of soot removal appeared near the forward part of the plate. Of interest in the photograph of figure 11 is the presence of soot in the corner. The flow model suggested from the observations shown in figure 11 is that separation was occurring at a distance 2-1/2 to 3 inches ahead of the step. Secondly, a vortex exists directly in front of the step with greater shearing action than is found in the unseparated boundary layer. The region directly in the corner between the flat plate and the step will be more evident in the heat-transfer measurements.

Figure 12 shows the flow field observed with the glow-probe technique. Although a direct interpretation of the photograph is questionable, roughly the regions of glow correspond to regions of density gradients. The glow is due to the collision of high-energy electrons with the gas molecules. The molecules radiate away the energy gained from the electron and produce the glow. Thus, the regions of glow must correspond to regions where a large number of electron-molecule collisions occur. The sketch on figure 12 outlines the approximate regions of glow in the flow field above the model. The region of glow back from the leading edge defines roughly the region between the expected two shock system setup by the separation. The inner edge of the glow makes an angle of roughly 4.5 degrees with the surface. The Mach angle for a Mach 14 flow is

4.096 degrees. A definite change in slope is evident in the glow band at a distance of about 3-1/2 inches. Extension of the line defined by the lower edge of the increased slope glow intersects the flat plate at 3 inches from the leading edge. Thus, the glow appears to define quite accurately the expected shock structure above the model. In all cases where pictures were obtained, the location of the glow regions were very repeatable. The region directly behind the separation shock is glowing in all cases. Photographs of radiation alone without the glow probe operating show only the slight glow seen at the upper part of the step.

In summary, the visual study of the flow over the flat-plate step model in the shock tunnel indicates that initial separation occurs at a distance of 3 inches ahead of the step. A region of high shear must also exist over a region of approximately 1 inch ahead of the step.

Figure 13 is a plot of the heat-transfer distribution for the flat plate shown in figure 3. The curve represents the flat-plate laminar boundary layer theory assuming equilibrium flow. The equation may be stated as follows:

$$Nu = 0.332 Re^{1/2} Pr^{1/3} ,$$

or

$$q = \frac{0.332 Re^{1/2} \mu (h_{ST} - h_W)}{Pr^{2/3} x} .$$

Agreement between the data points and the theory is close. A similar plot at a different running condition is shown in figure 14.

The distribution of heat transfer obtained from experiments in which a 1-inch-high step was placed on the flat plate 6 inches from the leading edge is shown in figure 15. The flat-plate laminar-boundary layer theory is also shown. Agreement between the data of figures 13 and 15, and the flat plate theory is good up to 3 inches from the leading edge. A high peak of 1.8 watts/cm<sup>2</sup> then appears, followed by a rapid fall to approximately 0.3 watt/cm<sup>2</sup> by the end of the next inch. The heat transfer then follows a steady rise, passing through the flat plate value at 5 inches from the leading edge and rising to a new peak of approximately two times the flat-plate value at a distance of 5.6 inches. In the remaining 0.4 inch the heat-transfer rate drops rapidly and finally becomes negative near the step.

A similar plot to that described above is shown in figure 16 for a different running condition and for fewer gage locations. The data points follow a similar trend to those discussed above.

The heat-transfer distribution on the face of the step is shown in figure 17. A high-heat-transfer rate is recorded near the top of the step, followed by a steady decrease as the plate is approached.

A flow pattern similar to that shown in figure 18 may be used to explain the heat-transfer distribution. Heat is transferred through the shear layer which marks the edge of the separated region and is carried into the region by the vortex. The highest heat-transfer rates would be expected in the region where the hot gas from the shear layer first meets the wall, and the lowest rates just before the gas is entrained into the shear layer after flowing around the vortex. With the exception of the negative heat rate recorded near the corner of the step, which cannot as yet be explained, the general trend of the heat-transfer data agrees with the description of the flow model. The high heat rate occurring near the separation point may be associated with the foot of the compression shock which will be present at the point of separation.

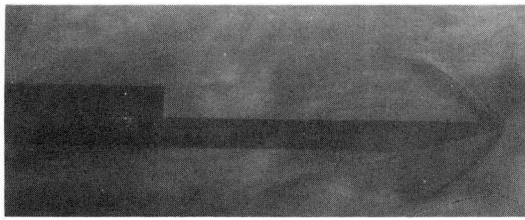
#### B. LOCAL HEAT-TRANSFER DISTRIBUTION ACROSS THE SEPARATED REGION

A complete understanding of the flow field above the separation model requires more information than is available from surface and visual measurements. Instrumentation to measure local flow properties in hypersonic shock tunnels is limited. Thus, it is not yet possible to measure, directly, velocity, density, or temperature profiles around the test model. To obtain some information on the flow field in the present experimental program, a hot-wire calorimeter has been developed. The measurements reported herein represent the preliminary results from the calorimeter. Basically, the data obtained can be interpreted similar to the surface heat-transfer measurements. The hot wire acts as a calorimeter in that it stores heat transferred to it from the flow. A correction must be made for the heat transferred from the wire to the supports. The actual reduction of the measurements and correction for end losses is outlined in the appendix.

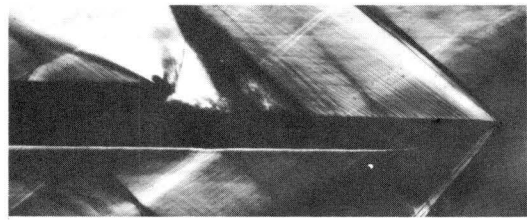
Figure 19 shows some typical traces obtained from the wires during the course of the measurements. A thin-film surface gage at approximately the same location as the probes is also shown in figure 19. An initial slope in the heat-transfer traces corresponds to the unseparated flow directly behind the initial shock. When the shock reflected from the step passes over the transducers, there is a definite change in the output. The film gage on the surface shows the greatest effect of the reflected shock. One of the wires was operating as an electron collector at the same time as the heat transfer was recorded, and its output is also shown on figure 19.

The values of local heat transfer computed from the wire outputs are plotted in figure 20. As the shock and shear layers are approached the heat-transfer rate increases by at least an order of magnitude. The present survey is too

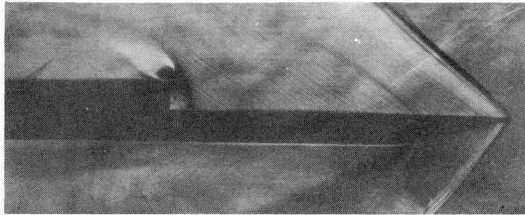
sketchy to define conditions right in the shear layer. However, the wire at 0.5 inch above the surface should be at least in the lower edge of the layer. (The wire locations are noted by small crosses on figure 12.) The wire at 1 inch above the surface was intended to be in the free stream, however the very high heat-transfer rate might suggest it is in the shock-wave region. The regions labeled in figure 20 were determined from the glow-probe data on figure 12. Actually the glow-probe data corresponds to the operating conditions for the heat-transfer data of figure 13, whereas the hot-wire data are for the conditions of figure 14. The slight variation in conditions were not expected to affect the shock structure, however, this point will require further investigation.



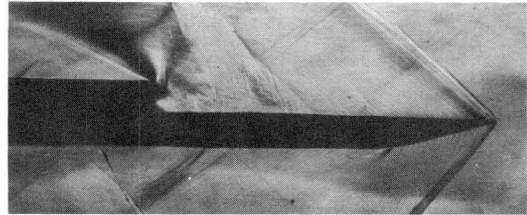
11  $\mu$  SEC  $M_S = 4.67$



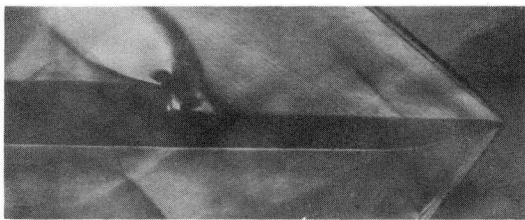
55  $\mu$  SEC  $M_S = 4.65$



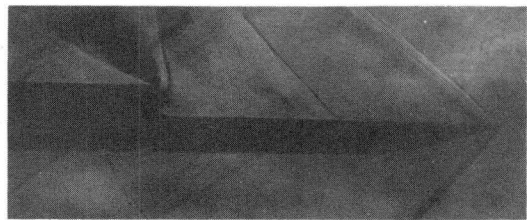
27  $\mu$  SEC  $M_S = 4.60$



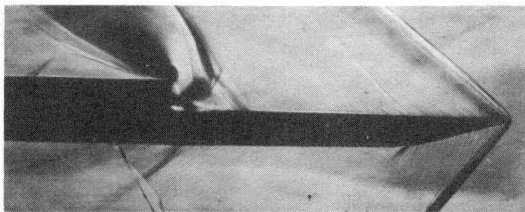
60  $\mu$  SEC  $M_S = 4.49$



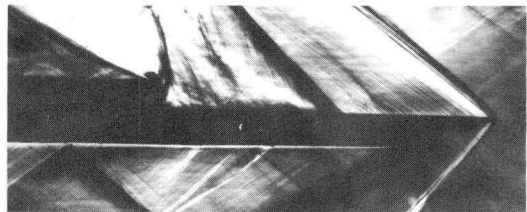
37  $\mu$  SEC  $M_S = 4.60$



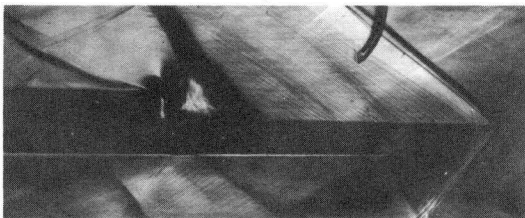
72  $\mu$  SEC  $M_S = 4.69$



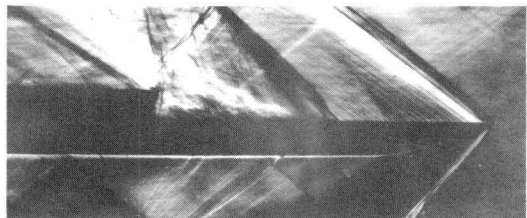
40  $\mu$  SEC  $M_S = 4.64$



90  $\mu$  SEC  $M_S = 4.60$



50  $\mu$  SEC  $M_S = 4.67$



130  $\mu$  SEC  $M_S = 4.67$

Figure 10 SCHLIEREN TIME HISTORY STUDY OF SEPARATION DEVELOPMENT  
63-5452

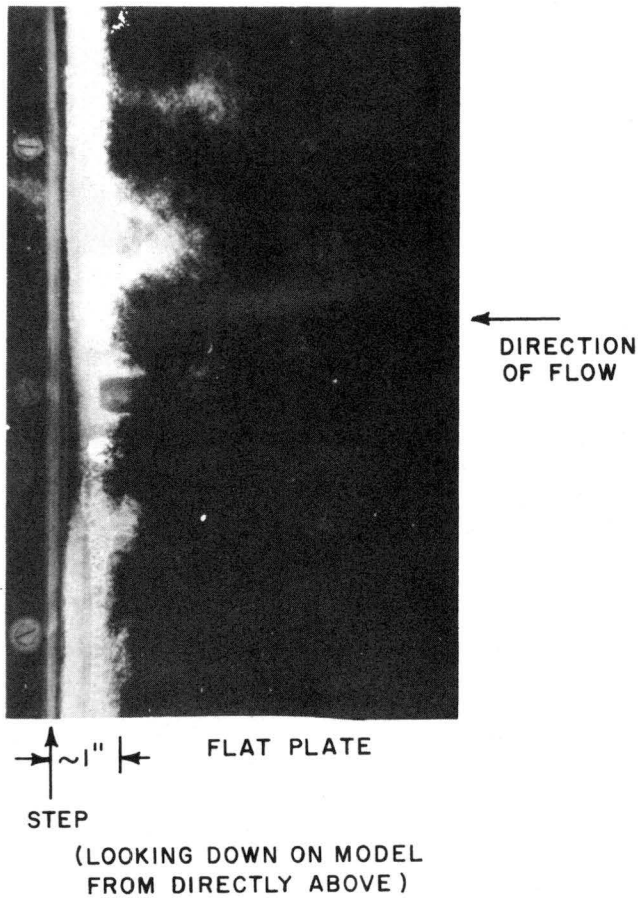
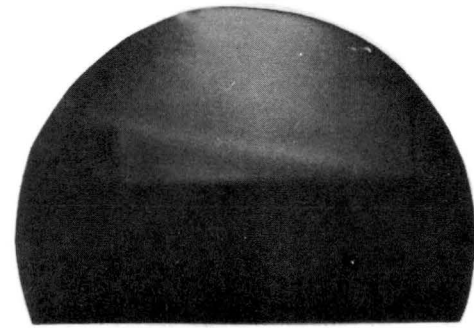


Figure 11 CARBON BLACK FLOW VISUALIZATION IN THE REGION OF THE  
STEP. SHOCK TUNNEL FLOW CONDITIONS  
63-5454



GLOW PROBE PHOTOGRAPH

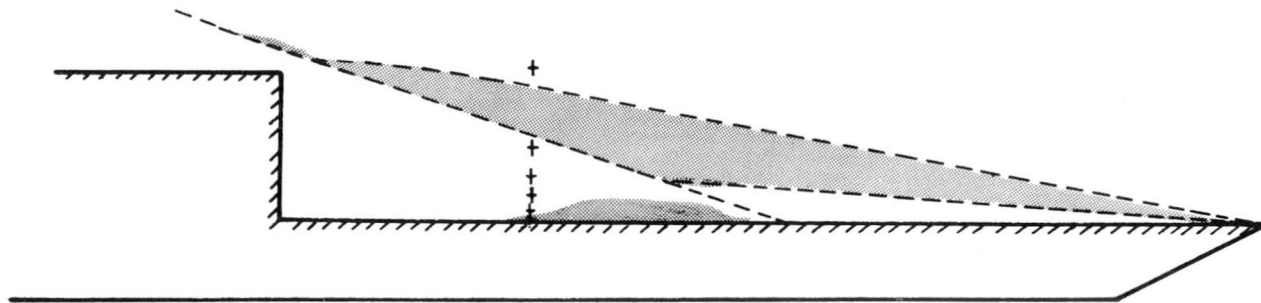


Figure 12 SHOCK WAVE STRUCTURE INDICATED FROM GLOW PROBE PHOTOGRAPH  
63-5455

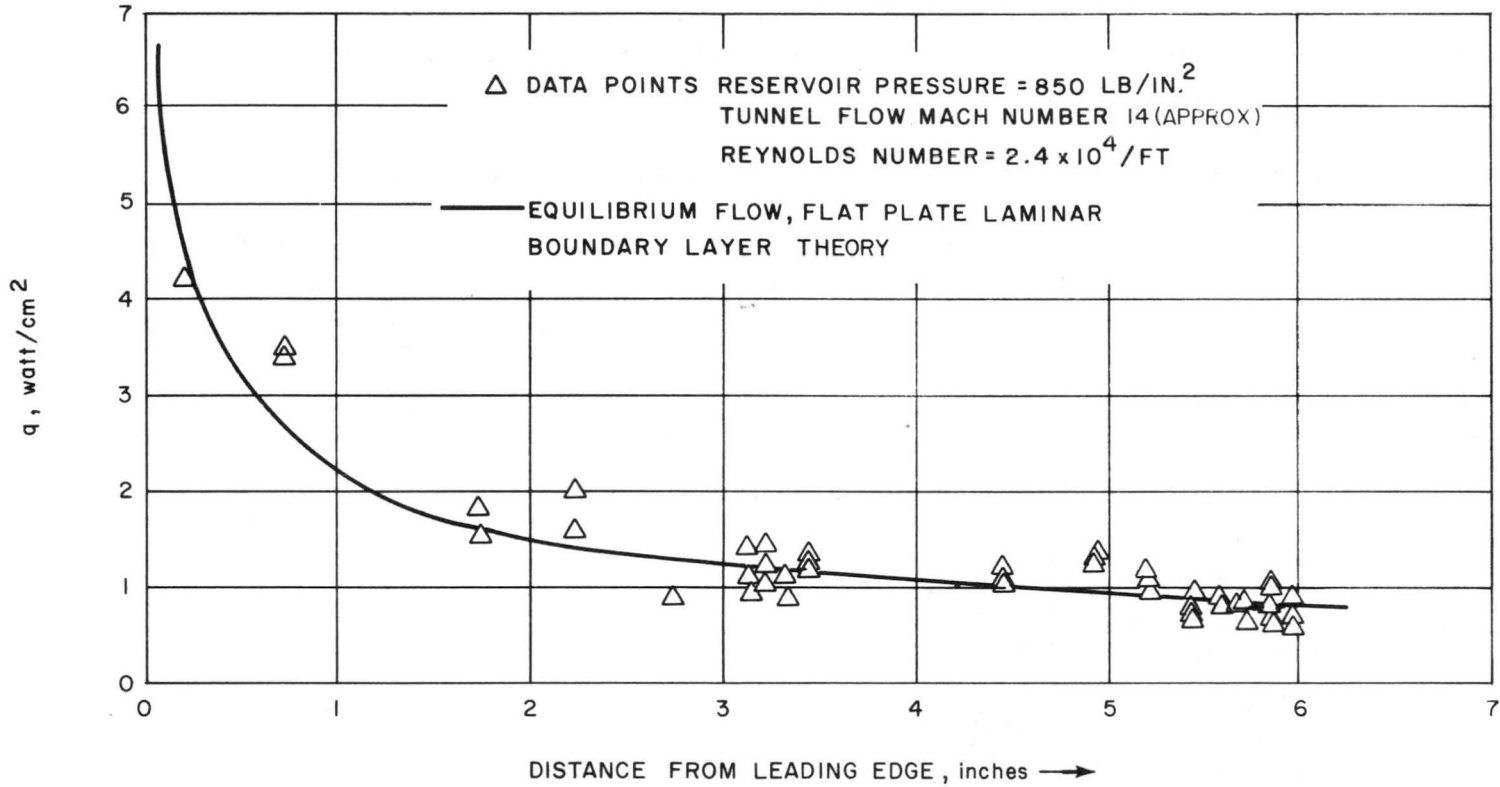


Figure 13 PLOT OF THEORETICAL AND EXPERIMENTAL HEAT TRANSFER  
DISTRIBUTION ON A FLAT PLATE  
63-5456

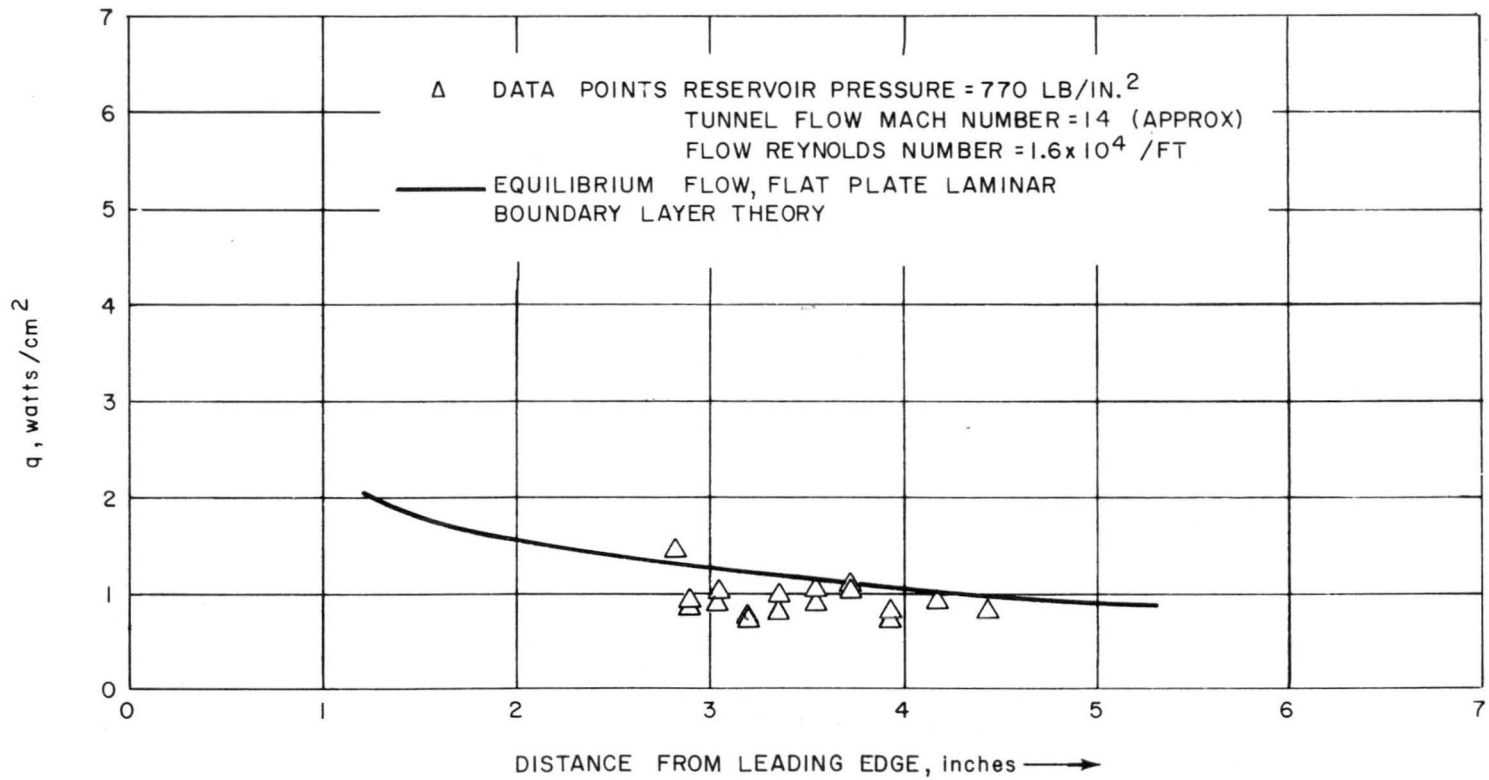


Figure 14 PLOT OF THEORETICAL AND EXPERIMENTAL HEAT TRANSFER  
DISTRIBUTION ON A FLAT PLATE  
63-5457

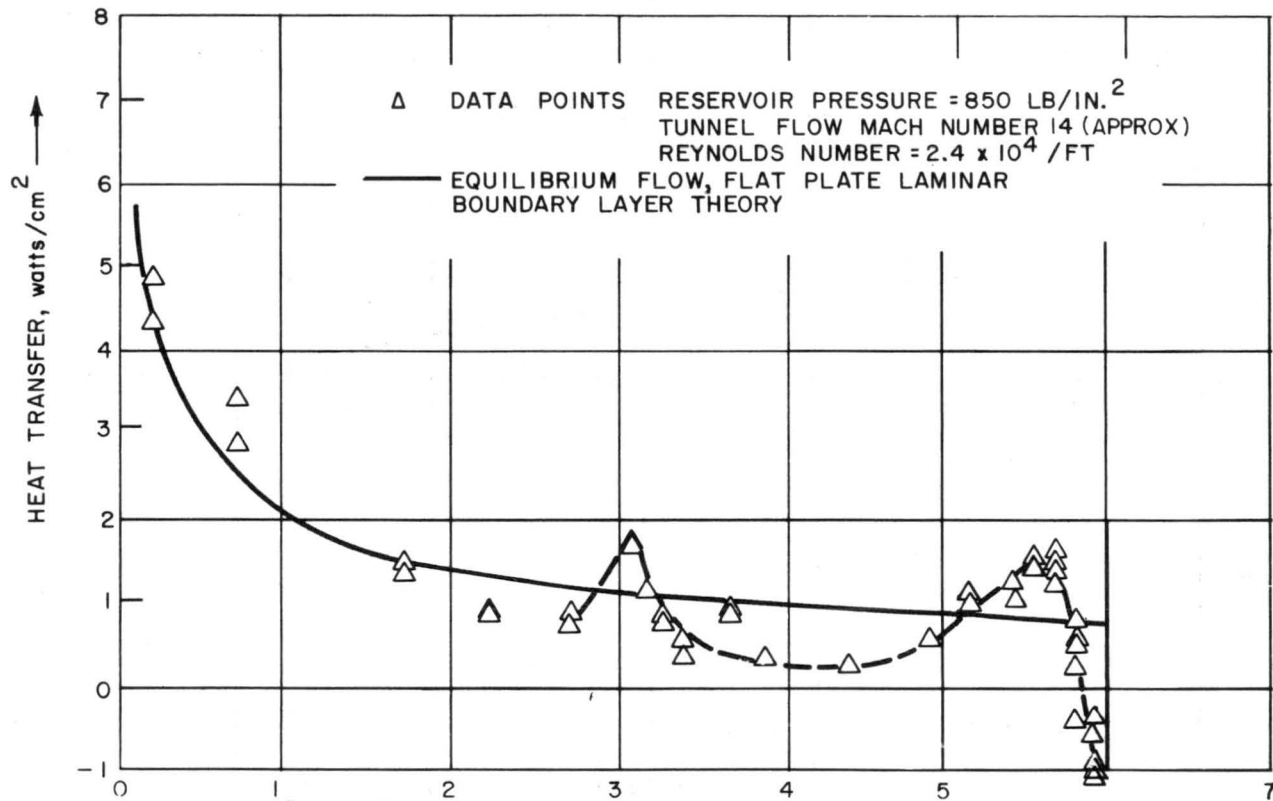


Figure 15 PLOT OF EXPERIMENTAL HEAT TRANSFER DISTRIBUTION ON A  
FLAT PLATE WITH STEP  
63-5458

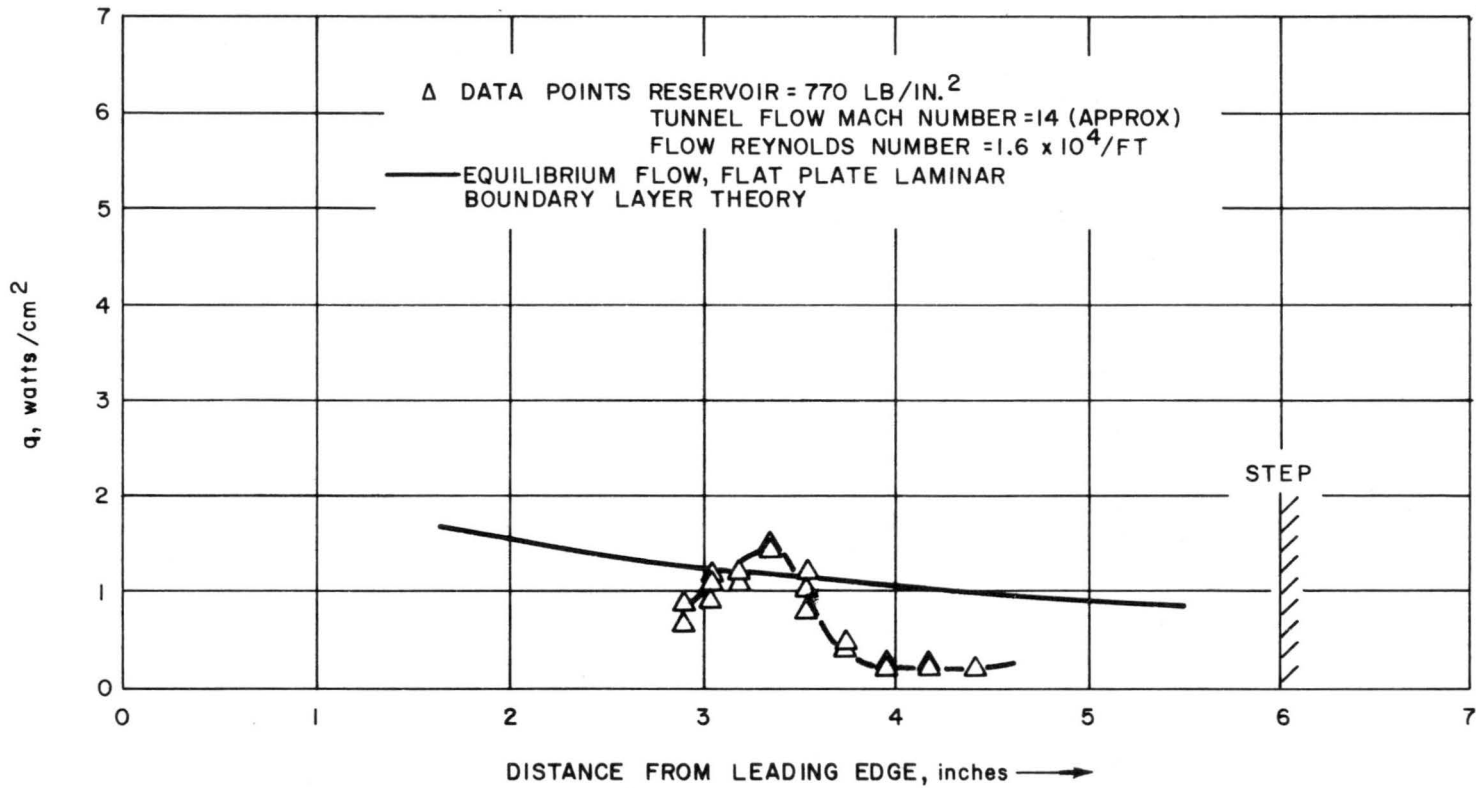


Figure 16 PLOT OF EXPERIMENTAL HEAT TRANSFER DISTRIBUTION ON A  
FLAT PLATE WITH A FORWARD FACING STEP  
63-5459

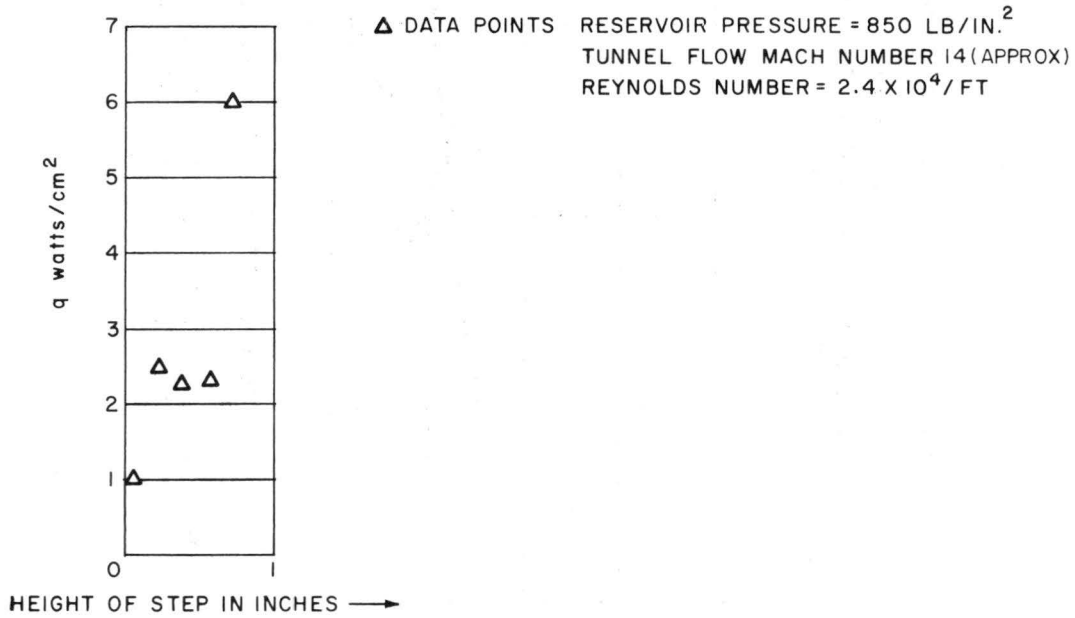
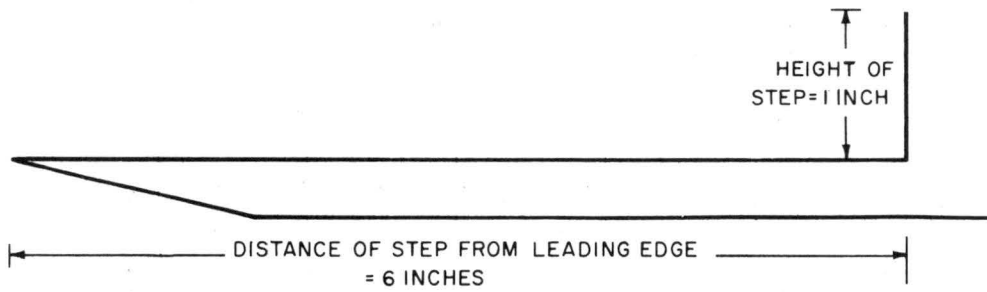


Figure 17 DISTRIBUTION OF HEAT TRANSFER ON FACE OF STEP  
63-5460

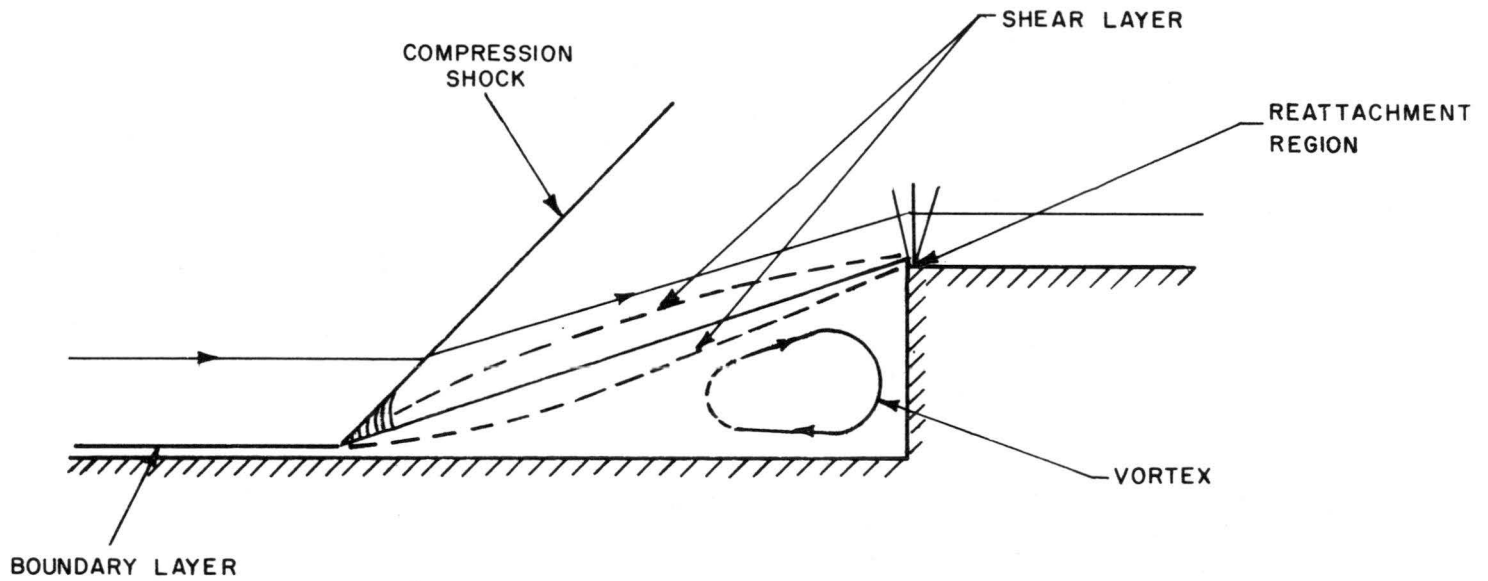


Figure 18 MODEL FLOW FIELD IN SEPARATED REGION  
63-5461

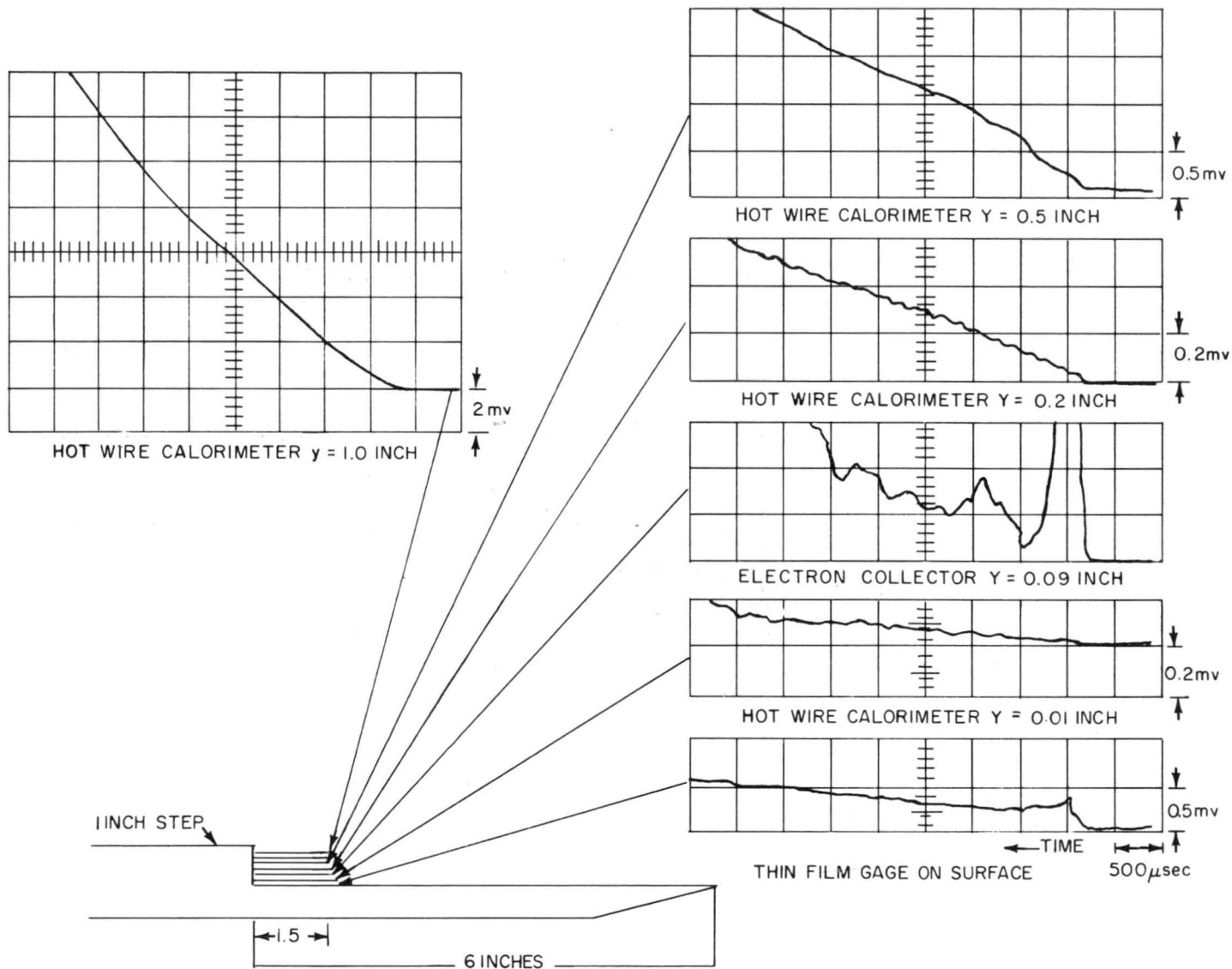
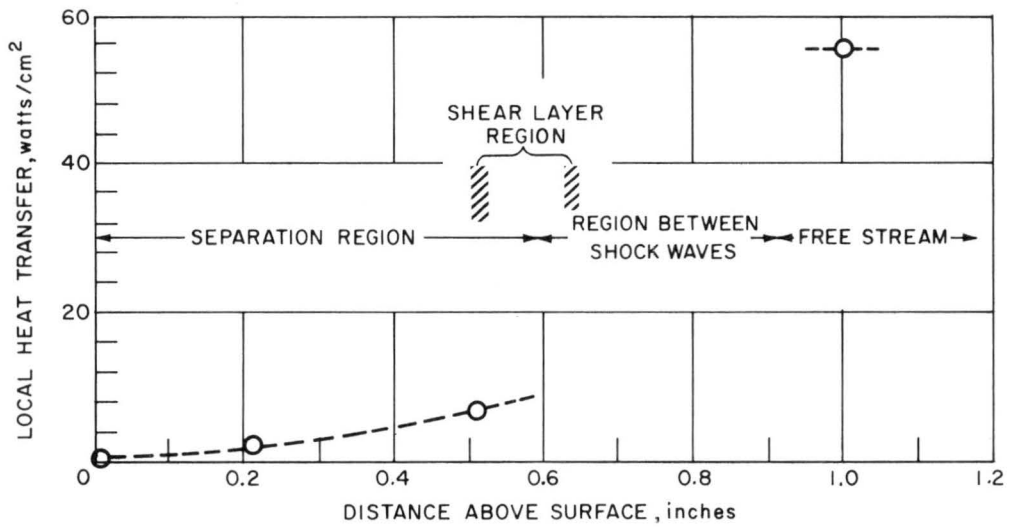
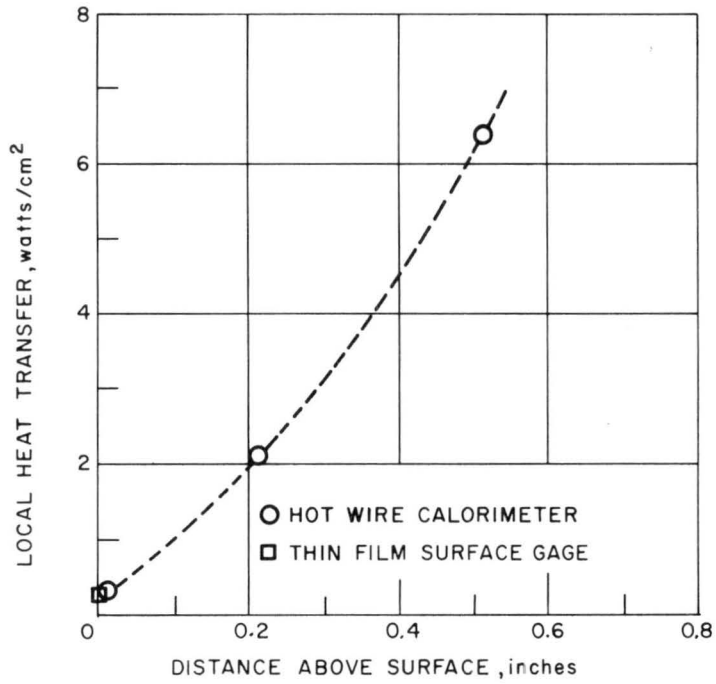


Figure 19 TYPICAL OUTPUT TRACES FROM THE HOT WIRE PROBES  
AND A HEAT GAGE  
63-5462



(a) COMPARISON OF FREE STREAM AND SEPARATED REGION



(b) SEPARATED REGION

Figure 20 MEASUREMENTS OF THE LOCAL HEAT TRANSFER ACROSS THE SEPARATED LAYER (1.5 INCHES AHEAD OF THE STEP)  
63-5463

#### IV. CONCLUDING REMARKS

The present report is viewed as an exploratory study of the separated flow field about a flat plate-step model. Only the thin-film heat-transfer gages have been used before in shock-tunnel measurements, so the data of the present report serves to establish a consistency for the new visual and calorimeter measuring techniques. These new techniques can now be utilized in more detailed studies of the separated flow field.

Detailed heat-transfer measurements on both the flat plate and the flat plate-step model are reported for two operating conditions. The flat-plate data are in good agreement with laminar-boundary layer predictions. The separation heat-transfer data show two regions of high-heat transfer. One region of very local extent occurs at the apparent location of the first point of separation, and the second high-heat-transfer rate occurs just ahead of the step. A peculiar "cold" region was discovered in the corner between the step and the flat plate.

## V. REFERENCES

1. Gortler, H., A new series for the calculation of steady laminar boundary-layer flows, *J. Math. Mech.* 6(1) (1957).
2. Tani, I., On the solution of the laminar boundary layer equations, *J. Phys. Soc. Japan*, 4(3) (1949).
3. Sandborn, V. A., and S. J. Kline, Flow models in boundary-layer stall inception. *J. Basic Engr. Trans. ASME, Ser. D.*, 83(3) (1961).
4. Glick, H. S., Modified Crocco-Lees mixing theory for supersonic separation and reattaching flows. *J. Aerospace Sci.*, 20 (10) pp 1238-1249 (1962).
5. Henshall, B. D., R. N. Teng, and A. D. Wood, Development of Very High Enthalpy Shock Tunnels with Extended Steady-State Test Time, Avco-RAD TR-62-16 (1962).
6. Peggs, P. J., K. Heron, H. Weisblatt, and A. Clemente, : Experimental Performance of the Avco RAD 20-inch Shock Tunnel, Avco RAD-TM-62-26 (1963).
7. Brown, H. K. The Theoretical Response of Heat Transfer Gages Employed in Shock Tubes, AERL, Research Note 58 (1958).
8. Henshall, B. D. and D. L. Schultz, Some Notes on the Use of Resistance Thermometers for the Measurement of Heat Transfer Rates in Shock Tubes, Aeronautical Research Council 20, 204 (1958).

## APPENDIX

### THE HOT-WIRE CALORIMETER

The hot-wire, resistance-temperature transducer has been used for many years as an anemometer. Recently,\* the calorimeter application of the transducer has been investigated in detail. The present application of the transducer for measurements in the separated region is actually a cross between the anemometer and calorimeter applications. The heat transfer will be a function of the flow properties; density, velocity, and temperature, and also of the transport properties; viscosity and thermal conductivity. With perhaps the exception of the wire at 1 inch above the plate, the temperature is expected to be the largest driving function. Thus, for the preliminary evaluation the instrument is viewed as a calorimeter.

The hot wire calorimeter is approximately a first order system, so its response to a step change in temperature will be a linear increasing resistance with time. The present analysis assumes that the varying temperature encountered, as the shock tunnel starts and the separation region develops, before the "steady" flow

is established does not affect the final value of  $\frac{\partial T}{\partial t}$ . The error due to this

simplifying assumption has not as yet been evaluated. The heat transfer from the gas to the wire is given by the relation

$$q_t = \frac{D}{4} \rho c \frac{\partial T}{\partial t} \quad (A-1)$$

The hot wire calorimeter is operated with a constant current circuit, so that voltage measured directly across the wire is related directly to the wire resistance. The wire resistance is in turn a function of the wire temperature. In the present analysis the wire is assumed to be a linear function of temperature, with a thermal coefficient of resistance,  $\alpha = 4 \times 10^{-3}/^\circ\text{K}$ . The relation between the voltage and temperature gradients is

$$\frac{\partial T}{\partial t} = \frac{\Delta E}{i \Delta t \alpha R_0} \quad (A-2)$$

The total heat transfer,  $q_t$ , must be equal to the input from the flow minus the amount conducted from the wire to the wire supports.

$$q_t = q - q_c \quad (A-3)$$

---

\* Baldwin, L.V., and V.A. Sandborn, Hot-Wire Calorimetry: Theory and Application to Ion Rocket Research, NASA TR-R98 (1961).

The conduction heat loss is given by the relation

$$q_c = -\frac{kD}{4} \frac{d^2 T}{dx^2} \quad (A-4)$$

The temperature distribution along the wire can be determined from the theoretical analysis.\* However, for the present application an approximate estimate of the end loss was employed. The heat transfer was measured at wire currents of 10, 15, and 30 milliamps. The indicated heat transfer was extrapolated back to a wire temperature equal to that of the supports. This is not considered to be a highly accurate method of correcting end losses, but it should be good to  $\pm 20$  percent, which appears to be the accuracy of the present measurements.

The present wires were larger in diameter and also shorter than the ideal length for the calorimeter application. Further measurements will employ 0.0002 inch diameter wires, 0.5 inch long to improve the measurements. The flow in the shock tunnel is so mild that no wire breakage is encountered, so that a long, small-diameter wire can be employed.

---

\*Ibid.

DISTRIBUTION

<u>Addressee</u>	<u>No. of Copies</u>
AFBSD, Attn: BSYDF, Lt. C. Hunter	2
AFBSD, Attn: BSTRA	1
AFBSD, Attn: BSRA, Capt. Lauritsen	1
Defense Documentation Center	10
AFSSD	
AF Unit Post Office	
Los Angeles, California	
Attn: Capt. Lewis, SSTRE	1
AFSSD	
AF Unit Post Office	
Los Angeles, California	
Attn: Lt. Col. Geniesse, SSGO-1	1
Aerospace Corporation	
San Bernardino, California	
Attn: H. Claflin	30
ARPA	
Washington 25, D. C.	
Attn: Lt. Col. McNamee	1
ARPA	
Washington, 25, D. C.	
Attn: C. E. McLain	1
ASD	
Wright-Patterson AFB, Ohio	
Attn: D. L. Schmidt, ASRNC-2	1
AFCRL	
L. G. Hanscom Field	
Bedford, Massachusetts	
Attn: N. W. Rosenberg, CRZAC	1
SAC (DORQ)	
Offutt AFB, Nebraska	1
AEDC (AES)	
Tullahoma, Tennessee	1
AMC (ORDAB-HT)	
Redstone Arsenal	
Huntsville, Alabama	1
ATIC (AFCIN-4BLA)	
Wright-Patterson AFB, Ohio	1
AUL	
Maxwell AFB, Alabama	1
Chief, DASA	
Washington 25, D. C.	1

DISTRIBUTION (Cont'd)

<u>Addressee</u>	<u>No. of Copies</u>
NASA, Ames Research Center Moffett Field, California	1
NASA, Lewis Research Center Cleveland, Ohio	1
NASA, Langley Research Center Virginia	1
Department of the Navy Washington, 25, D. C. Attn: SP-272	1
Central Intelligence Agency Washington, D. C. Attn: OCR-Std	2
BAMIRAC, University of Michigan Ann Arbor, Michigan Attn: R. Nichols	1
Batelle Memorial Institute Columbus, Ohio	1
Bendix Systems Division Ann Arbor, Michigan Attn: M. Katz	1
General Applied Science Laboratory Attn: M. Bloom	1
General Electric Company 3198 Chestnut Street Philadelphia, Pennsylvania	1
Hughes Aircraft Company Culver City, California Attn: E. Chrisler	1
Kaman Nuclear Garden of the Gods Road Colorado Springs, Colorado Attn: A. P. Bridges	1
Lincoln Laboratory, M. I. T. Lexington 73, Massachusetts Attn: F. McNamara	1
Los Alamos Scientific Laboratory Los Alamos, New Mexico	1
The RAND Corporation Santa Monica, California Attn: C. Gazley	1
AERL, Attn: R. Norling	1

DISTRIBUTION (Concl'd)

<u>Addressee</u>	<u>No. of Copies</u>
UCRL, "A" Division Livermore, California	1
Central Files	1
Document Control	5
Research Library	96